

OPTICAL PROPERTIES

Photoelectric, Nonlinear Optical, and Photorefractive Properties of Polymer Composites Including Carbon Nanotubes and Cyanine Dyes

A. V. Vannikov^{a,*}, A. D. Grishina^a, A. S. Laryushkin^a, T. V. Krivenko^a,
V. V. Savel'ev^a, and R. W. Rychwalski^b

^a *Frumkin Institute of Physical Chemistry and Electrochemistry, Russian Academy of Sciences, Leninskii pr. 31, Moscow, 199071 Russia*

* *e-mail: vanlab@online.ru*

^b *Department of Materials and Manufacturing Technology, Chalmers University of Technology, Göteborg, 416 96 Sweden*

Received July 23, 2012

Abstract—The effect of cyanine dye additives on the photoelectric, nonlinear optical, and photorefractive properties of polyvinyl carbazole composites based on closed single-walled carbon nanotubes has been investigated. It has been found that these characteristics are affected by the dye in which the lowest unoccupied molecular orbital (LUMO) lies below the level of the photoexcited nanotube. The addition of this dye to the composite leads to a 14-fold increase in the quantum efficiency of the generation of mobile charge carriers under irradiation by a laser (1064 nm) in the absorption region of the nanotubes. Moreover, the addition of the dye to the composite decreases the third-order susceptibility $\chi^{(3)}$, presumably, due to the opposite orientations of dipoles of the dye and the nanotube upon adsorption of the dye on the nanotube. The addition of the dye to the composite also provides a twofold increase in the two-beam photorefractive amplification factor of the laser beam with a wavelength of 1064 nm. The obtained values of the two-beam photorefractive amplification factor reach 120 cm^{-1} .

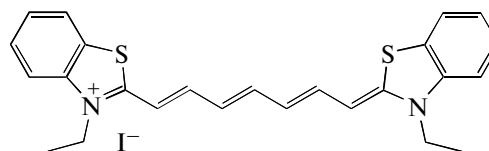
DOI: 10.1134/S106378341303030X

1. INTRODUCTION

This work continues the development of photorefractive materials based on polymers with a high glass transition temperature T_g . A high glass transition temperature improves the stability of the characteristics of the material, but requires using nanosized nonlinear optical chromophores with a significant third-order nonlinearity [1]. When polymer layers are obtained by coating from a solution, there appears a chaotic centrosymmetric distribution of orientations of the dipole moments of chromophores with any sizes. In rigid polymers, the applied direct-current (dc) electric field E_0 cannot change the orientation of the chromophores and ensure the orientation polarization. The second-order nonlinearity arises in a noncentrosymmetric distribution of chromophores. In the case of a chaotic orientation of chromophores, the third-order volume polarizability (susceptibility) differs from zero: $\chi^{(3)} = N\gamma f^4 \langle \cos^4 \xi \rangle$, because the average value is $\langle \cos^4 \xi \rangle = 1/5$. Here, ξ is the angle between the main axis of the chromophore and the direction of the polarization electric field, N is the concentration of chromophores, γ is the third-order molecular polarizability, $f = (n_0 + 2)/3$ is the Lorentz factor, and n_0 is the linear refractive index.

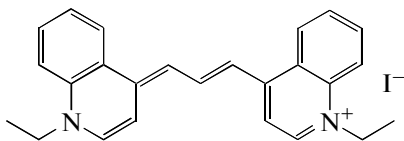
In this paper, we have considered the influence of cyanine dyes on the photoelectric, nonlinear optical, and photorefractive properties of the composite consisting of polyvinyl carbazole (PVK) and closed single-walled carbon nanotubes (SWCNTs). As will be shown below, SWCNTs are spectral sensitizers of the polymer composites to the fundamental absorption. This provides photogeneration of charge carriers and photorefractive sensitivity in the near-infrared region up to 2000 nm. Simultaneously, SWCNTs are third-order nonlinear optical chromophores.

Investigations have been performed using two dyes with differing positions of the HOMO–LUMO levels: 3,3'-diethylthiatriccyanine iodide (Dye 1)



with $\lambda_{\text{max}} = 760 \text{ nm}$, the electrochemical reduction potential $E_{\text{red}} = -0.78 \text{ V}$, and the oxidation potential $E_{\text{ox}} = 0.28 \text{ V}$ with respect to the saturated calomel

electrode (SCE); and 1,1'-diethyl-4,4'-decarbocyanine iodide (Dye 2)



with $\lambda_{\max} = 571$ nm, $E_{\text{red}} = -1.17$ V, and $E_{\text{ox}} = 0.90$ V. Since the Fermi level of the saturated calomel electrode is separated from the vacuum zero level by 4.64 eV [2], the LUMO levels correspond to 3.86 eV for Dye 1 and 3.47 eV for Dye 2.

2. SAMPLE PREPARATION AND EXPERIMENTAL TECHNIQUE

Electronic absorption spectra were recorded on a "Shimadzu UV-3101PC" scanning spectrophotometer for composites deposited on a quartz plate. The photoelectric and photorefractive characteristics of the composites were measured using a Nd : YAG continuous-wave laser emitting at a wavelength of 1064 nm. The composites were prepared as follows. First, SWCNTs were subjected to dispersion in tetrachloroethane for 30 min on an UZDN-A ultrasonic disperser. Then, the dye was added. The solution thus prepared was allowed to stand for 24 h. Thereafter, a solution of PVK ("Aldrich"; $M_w = 1.1 \times 10^6$; glass transition temperature is 200°C) in tetrachloroethane was added to the dispersion solution and stirred. The viscous mixture was again subjected to ultrasonic treatment for 5 min. The measurement cells were prepared as follows: first, in order to decrease the dark current, an Al_2O_3 dielectric film (band gap is 6.3 eV) was deposited on the electrode, i.e., the glass substrate coated with an $\text{In}_2\text{O}_3 : \text{SnO}_2$ (ITO) conducting layer. Then, the solution of the polymer composite was poured on the deposited film and dried for a long time at a temperature of 60°C. After the solvent was evaporated, first, the thickness of the composite was measured with an interferometer (the thickness of the photorefractive layer was 9.6–12.0 μm) and, then, a thin film of polyvinyl alcohol (PVA) was deposited on the composite in order to decrease the influence of oxygen. For measurements of the photorefractive properties after this procedure, the upper glass with the ITO electrode coated with the PVA thin film adsorbing molecular oxygen was pressed to the composite. The obtained cell was compressed under a low pressure at 60°C for 5 min. Then, the samples were placed in a vacuum chamber and stored before performing the measurements.

The photoelectric measurements were carried out after the determination of the photorefractive characteristics on the same samples. The upper electrode was removed, and the second electrode was prepared by depositing an opaque silver paste onto the area with a diameter of approximately 2.5 mm. The polymer layer

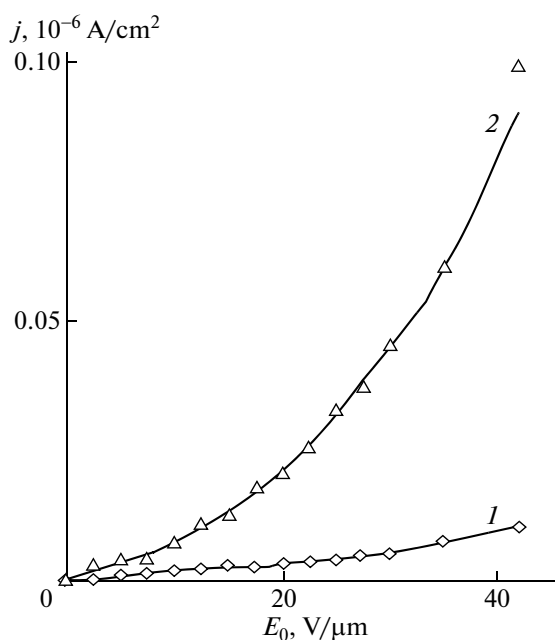


Fig. 1. Dependences of (1) the dark current j_d and (2) the photocurrent j_{ph} on the applied electric field E_0 in the PVK/SWCNT(0.26 wt %)/Dye 1(0.3 wt %) composite.

was illuminated by a single laser beam from the side of the ITO transparent electrode.

The third-order nonlinearity was measured using the z -scanning setup based on a pulsed femtosecond laser. The setup was fabricated as described in [3].

3. RESULTS AND DISCUSSION

The main measurements of the photovoltaic and photorefractive properties were performed on composites consisting of PVK, SWCNTs (0.26 wt %), and the dye (0.3 wt %). The long-wavelength optical absorption edge of Dye 1 lies in the region of 850 nm. The addition of this dye to the SWCNT solution did not lead to a change in the optical absorption at a wavelength of 1064 nm, but the fundamental absorption of the dye decreased by a factor of almost two after the 24-h holding of the solution in the presence of SWCNTs, most likely, as a result of the adsorption of the dye on the nanotubes.

3.1. Photoelectric Characteristics

The field dependence of the quantum efficiency of the generation of mobile charge carriers was estimated from the dependence of the photocurrent on the applied electric field $j_{\text{ph}}(E)$ at the radiation intensity of the Nd : YAG continuous wave laser $I_0 = 5.26$ W/cm². The photocurrent was estimated from the difference between the currents measured under irradiation $j_{\text{ph}} + j_d$ and in the dark j_d . Figure 1 shows the field depen-

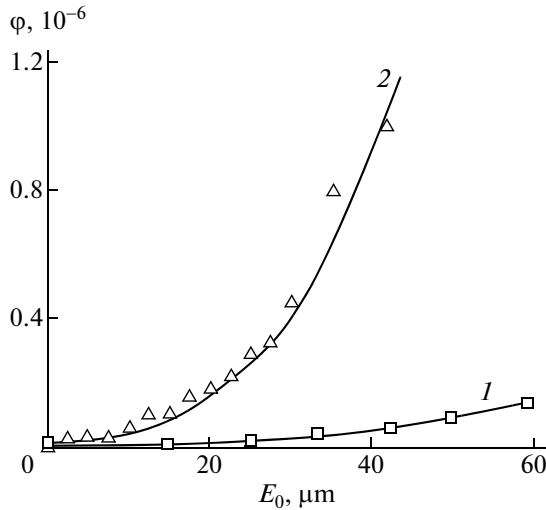


Fig. 2. Dependences of the quantum efficiency ϕ on the applied electric field E_0 in (1) PVK/SWCNT(0.26 wt %) composite and (2) composite with the additionally introduced Dye 1 (0.3 wt %).

dences of the steady-state photocurrent, i.e., the photocurrent obtained after the saturation was reached when the laser was turned off, and the dark current in the PVK/SWCNT 0.26 wt %) composites containing Dye 1 (0.3 wt %). The dependence of the quantum efficiency on the applied electric field $\phi(E_0)$ was calculated from the photocurrent $j_{ph}(E_0)$ according to the formula

$$\phi(E_0) = j_{ph}(E_0)hv/e[I_0(1 - \exp(-\alpha_0 d))]. \quad (1)$$

Here, $hv = 1240/1064 = 1.165$ eV ($hv/e = 1.165$ V). The quantity $(1 - \exp(-\alpha_0 d) = (1 - 10^{-4}) = (1 - \exp(-2.3A))$ is the fraction of the light energy absorbed in the layer. The optical density at a wavelength of 1064 nm is $A = 0.005$; therefore, the optical absorption coefficient is $\alpha = 2.3A/d = 9.6$ cm⁻¹, and the thickness of the layer is $d = 0.0012$ cm.

Figure 2 shows the dependences of the quantum efficiency on the applied electric field in the PVK/SWCNT composite without the dye (curve 1) and in the presence of Dye 1 (curve 2). It can be seen from this figure that the introduction of Dye 1 into the composite leads to a 14-fold increase in the quantum efficiency of the generation of mobile charge carriers under irradiation with light in the absorption region of SWCNTs at a wavelength of 1064 nm. The solid curves of the quantum efficiency in Fig. 2 are constructed using the Onsager equation

$$\phi(E_0) = \phi_0 P(r_0, E_0)$$

calculated to E_0^3 in the composites with the dye and to E_0^4 in the composites without the dye. Here, ϕ_0 is the quantum yield of thermalized electron-hole pairs

with the initial separation radius r_0 , and $P(r_0, E_0)$ is the probability that charge carriers in pairs will escape recombination at the separation radius r_0 [4]:

$$P(r_0, E_0) = \exp(-r_c/r_0) \{ [1 + (r_c/r_0)(eE_0 r_0/2kT) - (r_c/r_0)K_1(eE_0 r_0/2kT)^2 + (r_c/r_0)K_2(eE_0 r_0/2kT)^3 - (r_c/r_0)K_3(eE_0 r_0/2kT)^4] \}, \quad (2)$$

where

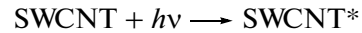
$$K_1 = [2 - (r_c/r_0)]/3,$$

$$K_2 = [1 - (r_c/r_0) + (r_c/r_0)^2/6]/2,$$

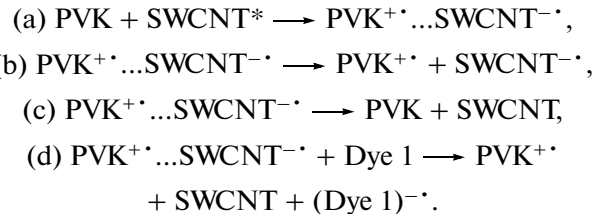
$$K_3 = [2 - 3(r_c/r_0) + (r_c/r_0)^2 - (r_c/r_0)^3/12]/15.$$

The solid curves in Fig. 2 are constructed according to Eq. (2) calculated to E_0^3 at $r_0 = 10.5$ Å and $\phi_0 = 0.5$ for the PVK/SWCNT(0.26 wt %)/Dye 1(0.3 wt %) composite (curve 2) and extended to E_0^4 at $r_0 = 9.8$ Å and $\phi_0 = 0.08$ for the PVK/SWCNT(0.26 wt %) composite without the dye (curve 1). In contrast to Dye 1, the addition of Dye 2 to the composite does not lead to an increase in the quantum efficiency of the composite consisting of PVK and SWCNT.

It is known [5] that electrically conducting polymers envelop SWCNTs in composite materials and interact with them. This leads to a significant increase in the charge carrier mobility in the polymer [5, 6]. The increase in the photocurrent after the addition of Dye 1 can be explained by the fact that the photoexcitation of SWCNT according to the reaction



results in the formation of geminate pairs $\text{PVK}^{+\cdot} \dots \text{SWCNT}^{-\cdot}$ according to reaction (a), which either partially decompose into free charge carriers (reaction (b)) or recombine according to reaction (c):



In accordance with the generally accepted concepts, Dye 1 plays the role of a sensitizer, because it limits (reaction (d)) the occurrence of the reverse reaction in the geminate pair (reaction (c)) by electron retransfer from $\text{SWCNT}^{-\cdot}$.

The mutual position of the work function of SWCNT, the excited level of SWCNT, and LUMO of Dye 1 and Dye 2 are presented in Fig. 3. When the energy levels are analyzed in experimental studies, the work function of SWCNT, as a rule, is taken to be equal to 5 eV [7]. As can be seen from Fig. 3, the electron

capture by Dye 1 according to reaction (d) is an energetically favorable process. It can also be seen from Fig. 3 that Dye 2 cannot provide the occurrence of reaction (d), because it is an activation process.

3.2. Nonlinear Optical Properties

The third-order nonlinearity was measured on a z -scanning setup based on a pulsed femtosecond laser. The schematic diagram of the experimental setup is presented in Fig. 4. The basic elements of the setup are as follows. Pulsed femtosecond laser Origami-10 (United States) 1 operates at the wavelength $\lambda = 1030$ nm. The laser radiation is modulated by a mechanical chopper placed at the focus of a Kepler telescope with a twofold magnification. The chopper is a rotating aluminum disk with two holes: the working hole with a large diameter is used to open the laser beam, and the hole with a small diameter is used to synchronize the operation of the measurement system with the rotation of the disk. The rotation frequency of the chopper is 50 Hz. The diameter of the large hole in the chopper is such that the laser beam is opened at ~ 470 μ s with a time of increase in the signal in the initial period of approximately 10 μ s. Next, the laser beam is focused by lens 2 with a focal distance of 6.5 cm. The movable unit allows sample 3 to be moved along the laser beam encompassing the prefocal ($-z$) region, the lens focus ($z = 0$), and the postfocal ($+z$) region (z -scanning). During the motion of the sample, the light transmission is measured in two modes: with diaphragm 4 (with an aperture of 0.1 cm at the diaphragm center) put on photodetector 5 (the closed aperture mode T_{CA}) and without the aperture (the open aperture mode T_{OA}). The laser pulse duration is 217 fs, and the pulse repetition rate is 74.82×10^6 s $^{-1}$. The average laser radiation power is 0.15 J/s. Therefore, the radiation energy per pulse is $0.15/(74.82 \times 10^6)$ J. For a pulse duration of 217 fs, the light power (per pulse) is $I = 9.24 \times 10^3$ W. The signal from the photodetector is amplified and recorded on a storage oscilloscope connected to a computer.

Owing to the high intensity of light in the focal region, there arise nonlinear optical effects: the refractive index increases from the linear value n_0 (for PVK, $n_0 = 1.5$) to the value

$$n = n_0 + n_2 I_0,$$

which, as is shown in Fig. 4, provides a phase shift $\Delta\Phi$, i.e., the displacement of the point of intersection of the beams from the lens focus into the prefocal region.

Curve 1 in Fig. 5 shows the dependence of the transmission T_{CA} on the distance to the focus ($z = 0$) in the solid composite of PVK and SWCNT(0.26 wt %). The experimental dependence of T_{CA} on z was fitted to the theoretical relationship [8]

$$T_{CA} = 1 - 4\Delta\Phi_0 x / [(x^2 + 1)(x^2 + 9)] \quad (3)$$

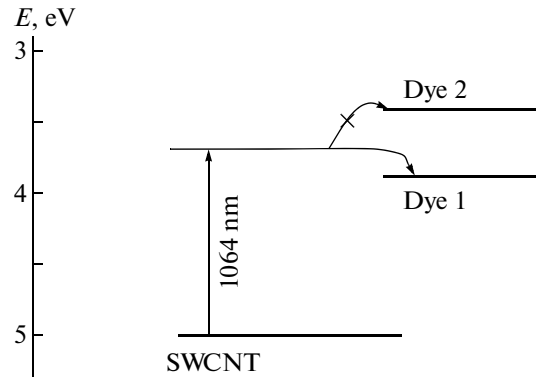


Fig. 3. Schematic diagram of the mutual position of the work function of SWCNT, the excited level of SWCNT, and LUMO of Dye 1 and Dye 2.

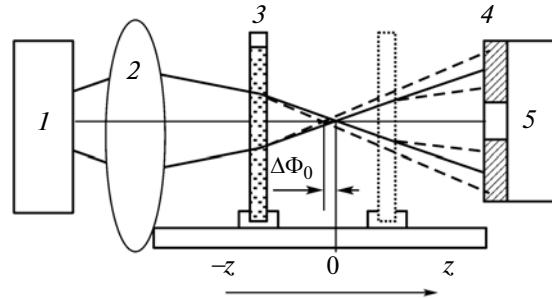


Fig. 4. Schematic diagram of the z -scanning setup: (1) pulsed femtosecond laser (1030 nm), (2) focusing lens, (3) moving sample, (4) diaphragm with an aperture of 1 mm, and (5) photodetector.

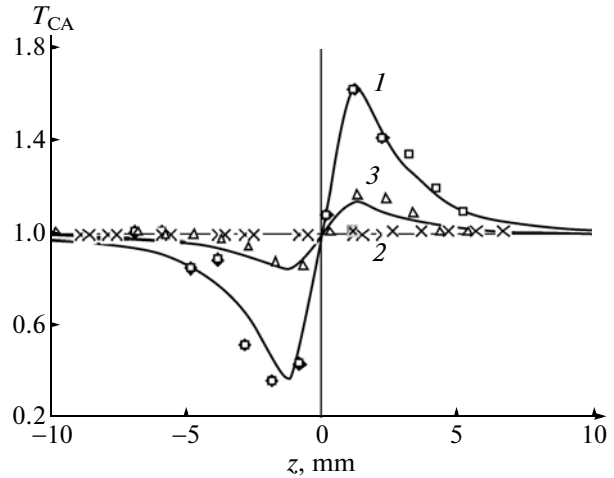


Fig. 5. Dependence of the transmission T_{CA} on the distance to the focus ($z = 0$). Experimental points are measured in (1) PVK/SWCNT(0.26 wt %) composite, (2) glass substrate, and (3) PVK/SWCNT(0.26 wt %)/Dye 1(0.3 wt %) composite. Solid curves show dependence (3) plotted for phase shifts $\Delta\Phi_0 =$ (1) 3.5 and (3) 0.7. The thickness of the composite is $L = 60$ μ m.

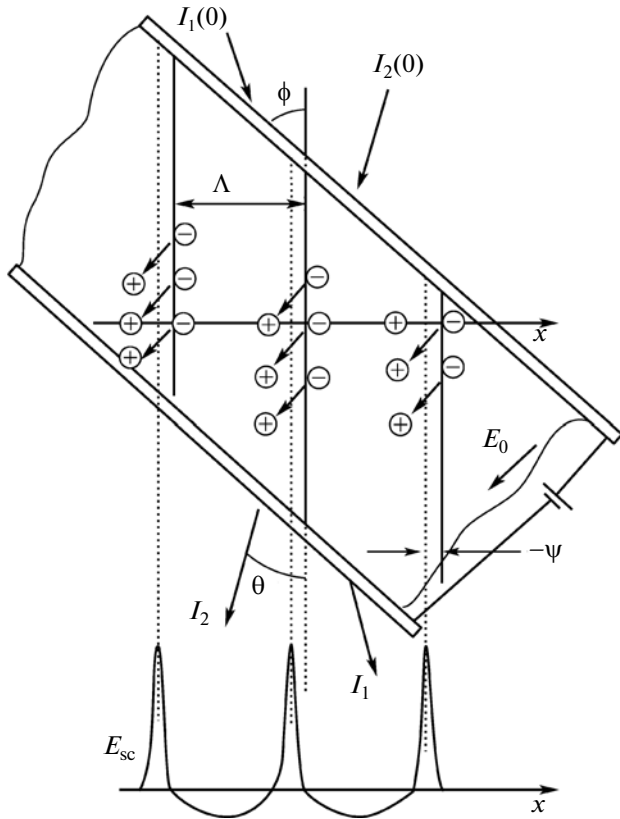


Fig. 6. Schematic diagram of the cell ITO/Al₂O₃/composite/PVA/ITO (from top to bottom) and the processes occurring during the measurement of the photorefractive effect. $I_1(0)$ and $I_2(0)$ are the intensities of the incident laser beams 1 and 2, respectively. Solid straight lines in the composite are interference fringes. Arrows inside the sample indicate the motion of holes in the electric field E_0 and the capture by traps. Dotted lines in the composite show the diffraction grating. The lower curve corresponds to the periodic space charge field E_{sc} .

by appropriately choosing the phase shift $\Delta\Phi_0$. Here, $x = z/z_0$ is the relative distance from the cell to the focus, and $z_0 = n_0\pi w_0^2/\lambda$ is the Rayleigh region, which, as known [9], is equal to the distance from the focus to the positions where the beam radius is $w_0 \times (2)^{0.5}$. The phase shift is related to the nonlinear effect $n_2 I_0$ by the expression [8, 9]

$$n_2 I_0 = \Delta\Phi_0 \lambda / 2\pi L_{\text{eff}}, \quad (4)$$

where $L_{\text{eff}} = (1 - e^{-\alpha_0 L})/\alpha_0$, L is the thickness of the composite, and α_0 is the optical absorption at a wavelength of 1030 nm. For $w_0 = 20.6 \mu\text{m}$, the length of the Rayleigh region is $z_0 = 1.94 \text{ mm}$.

In this work, we used the PVK layers with $L = 60 \mu\text{m}$. The optical absorption at a wavelength of 1030 nm is equal to $A = 0.025$; i.e., the optical absorption coefficient is $\alpha_0 = 9.6 \text{ cm}^{-1}$. Hence, we have $L_{\text{eff}} =$

0.00583 cm^{-1} . Solid curve 1 in Fig. 5 shows dependence (3) with the phase shift $\Delta\Phi_0 = 3.5$. From relationship (4), it follows that $n_2 I_0 = 0.0098$ and $n_2 = 1.42 \times 10^{-11}$. The real part of the third-order susceptibility is related to n_2 by the expression $\chi^{(3)} = n_2(n_0^2/0.0394)$ [esu]. Consequently, the PVK/SWCNT(0.26 wt %) composite has $\text{Re}\chi^{(3)} = 8 \times 10^{-10}$ esu. (Curve 2 in Fig. 5 corresponds to the transmission T_{CA} of the glass substrate.) The intense laser radiation induces two-photon optical transitions; therefore, in the focal region, the optical absorption coefficient includes the linear (α_0) and nonlinear (β) terms: $\alpha = \alpha_0 + \beta I_0$. The imaginary part of the third-order susceptibility is determined by the nonlinear absorption coefficient β and calculated using the formula [8, 9]

$$T_{OA} = [\ln(1 + q_0/(1 + x^2))]/[q_0/(1 + x^2)], \quad (5)$$

where $q_0 = \beta I_0 L_{\text{eff}}$. The experimental curve is approximated by relationship (5) for $q_0 = 1.3$. Therefore, $\beta = 1.3/I_0 L_{\text{eff}} = 1.9 \times 10^{-8} \text{ cm/W}$, and the imaginary part of the susceptibility is $\chi^{(3)} = (\beta\lambda/4\pi)(n_0^2/0.0394) = 0.9 \times 10^{-11}$ esu. Thus, the total susceptibility of the sample of the PVK/SWCNT(0.26 wt %) composite is predominantly determined by the real part of the susceptibility: $((\text{Re}\chi^{(3)})^2 + (\text{Im}\chi^{(3)})^2)^{0.5} = 8 \times 10^{-10}$ esu.

After the addition of the dye, the value of $\chi^{(3)}$ not only remains unchanged but even decreases by a factor of five, down to the value corresponding to $\Delta\Phi_0 = 0.7$ in relationship (3) (Fig. 5, curve 3), presumably, due to the opposite orientations of the dipoles of the dye and SWCNTs upon the adsorption of the dye on the nanotube.

3.3. Photorefractive Properties

The schematic diagram of the cell and the processes occurring during the measurement of the photorefractive effect is shown in Fig. 6. For the measurement of the photorefractive effect, the laser beam first is separated into beams 1 and 2, which then are brought together by mirrors and intersect with each other in the polymer layer, thus creating an interference pattern (Fig. 6). As is shown in Fig. 6, the angle between the beams is equal to $2\theta = 15^\circ$, and the slope of the bisector of this angle to the surface of the layer is $\phi = -45^\circ$. Beams 1 and 2 at the entrance to the layer have equal intensities $I_1(0) = I_2(0) = 0.12$ or 0.24 W/cm^2 . The sequence of operations used was as follows. First, object beam 2 was turned on; then, the direct-current (dc) electric field E_0 was applied. After that, beam 1 was turned on, and the interference emerged.

The photoexcitation of SWCNTs in the region of bright interference fringes results in the formation of electron-hole pairs with hole transfer to the polymer,

which, then, are separated according to reactions (b) and (d) and drift by hopping between carbazolyl groups of PVK in the dc electric field E_0 applied to the sample until they are captured by deep traps (Fig. 6, arrows inside the composite). The trapped electrons and holes form a periodic space-charge field E_{sc} (Fig. 6, lower curve). The polarization of SWCNT chromophores in the total field ($E_0 + E_{sc}$) provides a periodic modulation of the refractive index $\Delta n = (2\pi/n_0)\chi^{(3)}(E_0 + E_{sc})^2$; i.e., it creates the phase diffraction grating in the layer.

The photorefractive effect occurs only in the case when electrons and holes before the capture in traps are displaced to different distances from the site of generation. In the majority of electrically conducting polymeric materials, including PVK, holes are more mobile than electrons; therefore, the periodic space-charge field E_{sc} is shifted toward the direction of the hole motion. As is shown in Fig. 6, the maxima of the space-charge field and, therefore, the diffraction grating are shifted relative to the interference pattern at the distance $-\Delta x$ or the phase $-\psi = 2\pi\Delta x/\Lambda$, where Λ is the period of the diffraction grating. In this case, the transmitted laser beam, which is directed from the interference fringe to the diffraction grating (Fig. 6, object beam 2), coincides in direction and phase with the reflected part of the other, pumping beam 1; as a result, their constructive interference provides an enhancement of transmitted object beam 2. Pumping beam 1 is opposite in phase to the reflected part of object beam 2, and their destructive interference leads to extinction of the pumping beam.

The spatial period of the interference pattern at $\lambda = 1064$ nm is equal to $\Lambda = \lambda/(2n_0\sin\theta) = 2.7$ μm , because $\theta = 7.5^\circ$ and $n_0 = 1.5$. The diameter of the light spot in the region of the intersection of the incident beams $I_1(0)$ and $I_2(0)$ is close to 4.5 mm.

The two-beam photorefractive amplification factor Γ increases proportionally to Δn and $\sin\psi$:

$$\Gamma = 4\pi\Delta n \cos 2\theta \sin|\psi|/\lambda. \quad (6)$$

Figure 7a shows the kinetic curves of the two-beam coupling, which were measured in a dc electric field of 83.3 V/ μm and at laser radiation intensities $I_1(0) = I_2(0) = 0.12$ W/ cm^2 in the polymer composites PVK/SWCNT(0.26 wt %) (curve 1) and PVK/SWCNT(0.26 wt %)/Dye 1(0.3 wt %) (curve 2). The measurements were carried out according to the following scheme. First, beam 2 was turned on (in Fig. 7a, the intensity of this beam at the exit from the layer is designated as I_{20}), and the negative potential was applied to the output electrode so that, in the sample, it created the dc electric field E_0 directed from the input electrode (anode) to the output electrode (cathode) (Fig. 6). Then, at the instant of time indicated by the upward arrow, beam 1 was turned on. As can be seen from Fig. 7a, this turning on led to an increase in

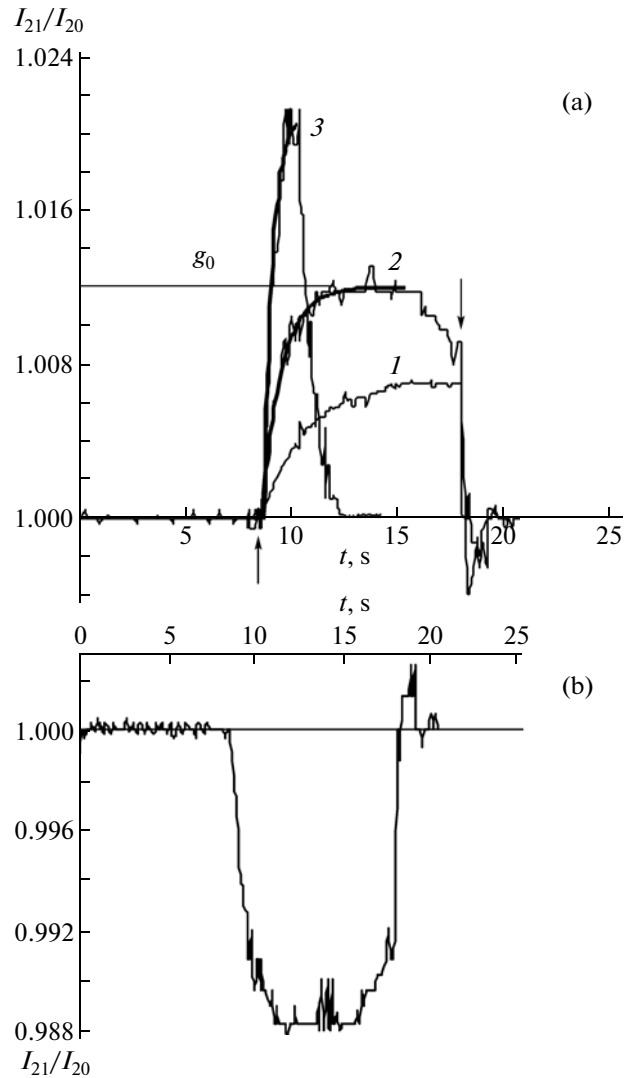


Fig. 7. (a) Kinetic curves of the two-beam coupling in (1) PVK/SWCNT(0.26 wt %) polymer composite, (2) PVK/SWCNT(0.26 wt %)/Dye 1(0.3 wt %) composite, and (3) composite after a 3-min preliminary irradiation at 633 nm. The applied dc electric field is $E_0 = 83.3$ V/ μm . The laser intensities are $I_1(0) = I_2(0) = 0.12$ W/ cm^2 . (b) Mirror reflection of curve 2 in panel (a).

the intensity of beam 2 (under conditions of operation of beam 1, the intensity of beam 2 is designated as I_{21}). A few seconds after the intensity of beam 2 reached saturation (or the maximum), beam 1 was turned off (in Fig. 7a, this instant of time is indicated by the downward arrow), and the intensity of beam 2 took on the initial value I_{20} . It is shown using experimental curve 2 as an example that an increase in the ratio I_{21}/I_{20} is adequately described by the equation

$$I_{21}/I_{20} = 1 + (g_0 - 1) \{1 - \exp[-(t - t_0)/\tau]\}.$$

Here, g_0 is the amplification factor equal to the ratio I_{21}/I_{20} at saturation of the kinetic curve, and τ is the

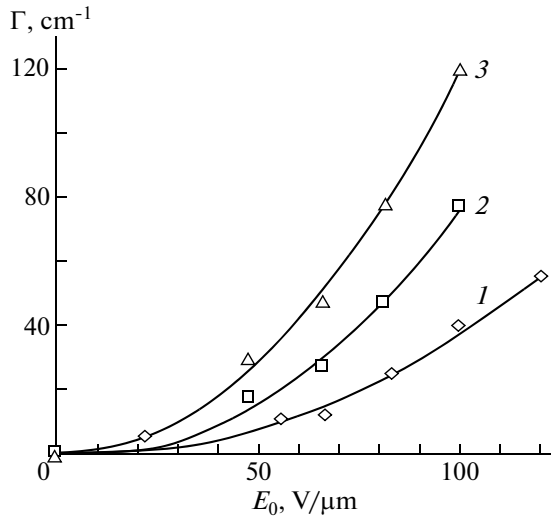


Fig. 8. Field dependences of the two-beam photorefractive amplification factor Γ at intensities $I(0)_1 = I(0)_2 = I$ 0.12 and (2, 3) 0.24 W/cm² measured (2) without preliminary irradiation and (3) with preliminary irradiation.

response time (the time constant of the formation of the diffraction grating). Curves 1 and 2 shown in Fig. 7a have the parameters $g_0 = 1.006$, $\tau = 2$ s and $g_0 = 1.012$, $\tau = 0.9$ s, respectively; i.e., the introduction of the dye into the composite provides a twofold increase in the amplification factor.

Curve 3 shown in Fig. 7a was measured on the sample whose surface was preliminarily entirely irradiated with light from the continuous wave laser at a wavelength of 633 nm in the absorption region of the dye. The irradiation of the sample surface was performed with an intensity of 0.1 W/cm² for 3 min in the absence of an electric field. It can be seen that such a preliminary irradiation leads to an additional twofold increase in the amplification factor (to the parameters $g_0 = 1.024$ and $\tau = 0.4$ s). This increase can be attributed to the charge carrier photogeneration and filling of deep hole traps under the preliminary irradiation, which, under conditions of the subsequent interference at a wavelength of 1064 nm, provides an increase in the mean free path of free holes, until they are captured by traps, and an increase in the two-beam photorefractive amplification factor Γ due to the increase in the phase shift ψ (Fig. 6). It can be seen from Fig. 7a that, in the presence of Dye 1, during the writing of the diffraction grating, the intensity I_{21} first increases, reaches a maximum, and then decreases. This effect is particularly pronounced after the preliminary irradiation of the sample. It can be associated with a gradual decrease in the dc electric field E_0 inside the sample due to the accumulation of the space charge upon the passage of the dark current. In order to exclude the effect of the space charge, the curves were alternately recorded with a change in the polarity of the electrodes. When

the direction of the applied electric field changed oppositely to that shown in Fig. 6 (the anode and cathode exchanged their places), the intensity of beam 2, as shown in Fig. 7b, decreased according to the relationship

$$I_{21}/I_{20} = 1 - (g_0 - 1)\{1 - \exp[-(t - t_0)/\tau]\};$$

simultaneously, the intensity of beam 1 increased. This change indicates a photorefractive nature of the effect and results from the displacement of the diffraction grating (Fig. 6, dashed straight lines inside the layer) from the position to the left of the interference fringe to the position to right of it. The curve shown in Fig. 7b is a mirror image of curve 2 in Fig. 7a, and the parameters of these curves coincide.

Figure 8 shows the field dependences of the two-beam photorefractive amplification factor Γ for the PVK/SWCNT(0.26 wt %)/Dye 1(0.3 wt %) composite, which was calculated from the standard formula

$$\Gamma = [LN(g_0\beta/(1 + \beta - g_0))]/L.$$

Here, $\beta = I(0)_1/I(0)_2$ and $L = d/\cos(\phi - \theta)$ is the optical path of beam 2 (Fig. 6). These dependences were measured at the intensities $I(0)_1 = I(0)_2 = 0.12$ (curve 1) and 0.24 W/cm² (curve 2). As can be seen from Fig. 8, the increase in the laser radiation intensity leads to a nearly twofold increase in the two-beam amplification factor. For $E_0 = 100$ V/μm and $I(0)_1 = I(0)_2 = 0.24$ W/cm², the two-beam photorefractive amplification factor and the efficiency are $\Gamma = 80$ cm⁻¹ and $\Gamma - \alpha = 70.4$ cm⁻¹, respectively. Under conditions of the preliminary irradiation (curve 3), these parameters increase to $\Gamma = 120$ cm⁻¹ and $\Gamma - \alpha = 110.4$ cm⁻¹.

For the PVK/SWCNT(0.26 wt %)/Dye 1(0.3 wt %) composite, we measured the dependence of the amplification factor on the intensity ratio of the pumping and object beams $\beta = I_1(0)/I_2(0)$. An increase in β was achieved by the decrease in the intensity of object beam $I_2(0)$. Figure 9 shows this dependence measured in the field $E_0 = 66$ V/μm. It can be seen from this figure that the amplification factor Γ initially increases from 27 to 66 cm⁻¹ with an increase in β from 1 to 1.66 and then slowly decreases. This effect is of great practical importance, because it makes possible correction of an image transmitted by IR rays. Indeed, if a partially veiled image, which contains regions where the intensity $I_2(0)$ is decreased from $I_2(0) = I_1(0)$ to $I_2(0) = I_1(0)/a$ (where a varies in the range from 1 to 1.66), is projected by beam 2 onto the photorefractive layer, then, after the passage through the photorefractive layer, the veil effect is weakened, because, in accordance with the shape of the curve (Fig. 9), the intensity of beam 2 in these regions increases.

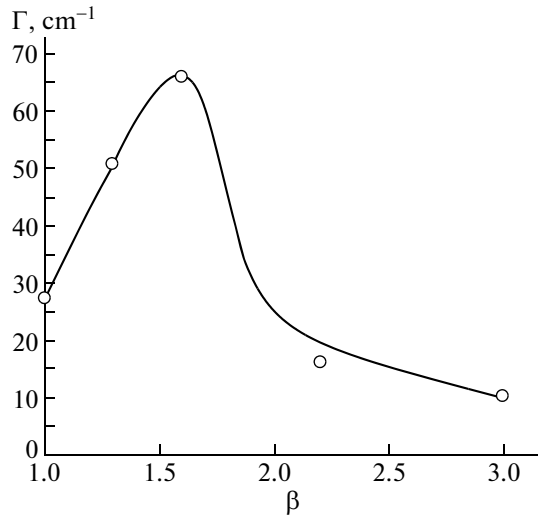


Fig. 9. Dependence of the two-beam photorefractive amplification factor on the intensity ratio of the pumping beam and the objective beam $\beta = I_1(0)/I_2(0)$ in the PVK/SWCNT(0.26 wt %)/Dye 1(0.3 wt %) composite. The applied dc electric field is $E_0 = 66 \text{ V}/\mu\text{m}$.

3.4. Diffraction Efficiency

The measurement of the diffraction efficiency η makes it possible to estimate the modulation of the refractive index Δn , which is related to η by the expression

$$\eta = \sin^2(\Delta n \pi d \cos 2\theta) / \lambda [\cos(\phi - \theta) \cos(\phi + \theta)]^{0.5}, \quad (7)$$

and, with the known value of the two-beam photorefractive amplification factor Γ , to determine the phase shift ψ according to formula (6). The diffraction efficiency was measured in the sample of the composite PVK/SWCNT(0.26 wt %)/Dye 1(0.3 wt %) with a layer thickness of $9.6 \mu\text{m}$ in the dc electric field $E_0 = 83.3 \text{ V}/\mu\text{m}$ during the writing of the diffraction pattern by a laser (1064 nm), $I(0)_1 = I(0)_2 = 0.12 \text{ W}/\text{cm}^2$. The third beam emitted by a He–Ne laser at a wavelength of 633 nm was used as a reading beam. This beam crossed the sample parallel to beam 1 (at the cell output, beam 1 was blocked by IR filters). Since the composite in this region exhibited a photoelectric sensitivity, the initial intensity of the third beam was decreased to $I_{30} = 0.02 \text{ mW}/\text{cm}^2$. We measured the decrease in the intensity of transmitted beam I_3 due to the diffraction during the formation of a diffraction grating. The diffraction efficiency η was measured under the conditions where first the detected beam 3 was turned on, then, the dc electric field E_0 was turned on, and, a few seconds later, at once both beams (beams 1 and 2) were turned on, which wrote the diffraction grating at a wavelength of 1064 nm. After a few seconds, the dc electric field E_0 was turned off and the intensity I_3 returned to the initial value I_{30} . It was found that $\eta = 0.018$ (1.8%). Hence, the modulation of the refractive

index calculated from formula (7) is close to $\Delta n = 0.0027$. The response time $\tau = 0.9 \text{ s}$ coincides with that obtained in the measurement of the amplification factor g_0 (Fig. 7a). Since under these conditions the two-beam photorefractive amplification factor is $\Gamma = 24 \text{ cm}^{-1}$, according to formula (6), the phase shift is $\psi = 5^\circ$. In the simultaneously coated samples in the absence of the dye, the diffraction efficiency decreases by a factor of approximately three, $\Delta n = 0.0015$ and $\psi = 3^\circ$.

Thus, a significant increase in the amplification factor g_0 upon introduction of Dye 1 into the composite is associated both with an increase in the mean free path of the hole, until it is captured by a trap (i.e., with an increase of the phase shift ψ) and with an increase in the modulation of the refractive index Δn , which is determined by the number of trapped charge carriers.

4. CONCLUSIONS

Photorefractive properties are inherent in polymer composites that exhibit a photoelectric sensitivity and nonlinear optical properties. In this work, carbon nanotubes have been used as spectral sensitizers of the PVK/SWCNT composites to laser irradiation at a wavelength of 1064 nm. Simultaneously, SWCNTs are responsible for the third-order nonlinear optical properties. The influence of the cyanine dye on the photoelectric, photorefractive, and nonlinear optical properties of the PVK/SWCNT/Dye composite has been investigated.

Dye 1 with the long-wavelength optical absorption edge near 850 nm serves as a supersensitizer. The addition of Dye 1 to the composite leads to a 14-fold increase in the quantum efficiency of the generation of mobile charge carriers under irradiation with light in the absorption region of SWCNTs at a wavelength of 1064 nm. Since the LUMO of Dye 1 lies below the level of the photoexcited nanotubes, this dye limits the reverse reaction in the process of charge phototransfer from PVK to the photoexcited nanotube by electron retrapping from SWCNT $^{-\cdot}$. Moreover, the capture of an electron by the dye decreases the electron mean free path, which leads to an increase in the phase shift ψ in the direction of the hole motion.

The addition of the dye to the PVK/SWCNT composite leads to a fivefold decrease in the third-order susceptibility $\chi^{(3)}$, most likely, due to the opposite orientations of the dipoles of the dye and SWCNTs upon adsorption of the dye on the nanotube.

The addition of Dye 1 to the composite provides a twofold increase in the two-beam photorefractive amplification factor of the laser beam with a wavelength of 1064 nm. For $E_0 = 100 \text{ V}/\mu\text{m}$ and $I(0)_1 = I(0)_2 = 0.24 \text{ W}/\text{cm}^2$, the two-beam photorefractive amplification factor and the efficiency are $\Gamma = 80 \text{ cm}^{-1}$ and $\Gamma - \alpha = 70.4 \text{ cm}^{-1}$, respectively. Under the condi-

tions of preliminary irradiation, these parameters increase to $\Gamma = 120 \text{ cm}^{-1}$ and $\Gamma - \alpha = 110.4 \text{ cm}^{-1}$.

ACKNOWLEDGMENTS

This study was supported by the Russian Foundation for Basic Research (project no. 11-03-00260) and Swedish Foundation for Strategic Research (SSF).

REFERENCES

1. M. G. Kусyk, Phys. Rev. Lett. **85**, 1218 (2000).
2. Yu. V. Pleskov and Yu. Ya. Gurevich, *Semiconductor Photoelectrochemistry* (Consultants Bureau, New York, 1986).
3. A. Gnoli, L. Razzari, and M. Righini, Opt. Express **13**, 7976 (2005).
4. A. Mozumder, J. Chem. Phys. **60**, 4300 (1974).
5. A. B. Dalton, J. N. Coleman, M. in het Panhuis, B. McCarthy, A. Drury, W. J. Blau, B. Paci, J.-M. Nunzi, and H. J. Byrne, J. Photochem. Photobiol., A **144**, 31 (2001).
6. A. R. Tameev, L. Ya. Pereshivko, and A. V. Vannikov, Polym. Sci., Ser. A **51** (2), 182 (2009).
7. A. Du Pasquier, H. E. Unalan, A. Kanwal, S. Miller, and M. Chhowalla, Appl. Phys. Lett. **87**, 203 511 (2005).
8. M. Sheik-Bahae, A. A. Said, T.-H. Wei, D. J. Hagan, and E. W. Van Stryland, IEEE J. Quantum Electron. **26**, 760 (1990).
9. R. L. Sutherland, *Handbook of Nonlinear Optics* (Marcel Dekker, New York, 1996).

Translated by O. Borovik-Romanova